

# Highly sensitive curvature sensor based on singlemode-multimode-singlemode fiber structures

SHAOHUA DONG, SHENGLI PU\*, AND JUAN HUANG

*College of Science, University of Shanghai for Science and Technology, Shanghai 200093, China*

A kind of highly sensitive curvature sensor based on singlemode-multimode-singlemode (SMS) fiber structure is demonstrated. The wavelength or intensity of the interference valley may vary with the curvature remarkably, which can be utilized for curvature sensing. The wavelength shift of the SMS structure with 26 mm-long multimode fiber (MMF) is very sensitive to the curvature. The measurement sensitivity of  $-13.17 \text{ nm/m}^{-1}$  is obtained in the curvature range of  $0.60\text{-}1.55 \text{ m}^{-1}$ . While for the SMS structure with 48 mm-long MMF, the intensity rather than the wavelength shift of the interference valley is very sensitive to the curvature. The measurement sensitivity of  $24.64 \text{ dB/m}^{-1}$  in the curvature range of  $0.22\text{-}0.89 \text{ m}^{-1}$  is achieved.

(Received August 21, 2014; accepted November 13, 2014)

*Keywords:* Optical fiber sensor, Curvature, SMS, Mode interference

## 1. Introduction

Fiber-optic sensors have already been widely utilized in different areas for the measurement of many physical parameters including temperature, refractive index, magnetic field [1-3], chemical concentration and gas [4, 5] and so on. These are assigned to their compact size, high sensitivity, fast response, good stability and repeatability. Special attention has been paid to the development of fiber curvature sensors which have many applications in the fields of composite material structure, robot arms and artificial limbs and so on. A number of optic fiber curvature sensors have been proposed based on different optical fiber structures, such as photonic crystal fiber (PCF) [6], PCF based Mach-Zehnder interferometers [7, 8], polarization-maintaining PCF [9, 10], polarization maintaining fiber (PMF) [11], long-period fiber gratings (LPFGs) [12, 13], tilted-fiber Bragg gratings (TFBGs) [14, 15] and two-dimensional waveguide array fiber (WAF) [16]. Though many promising results have been achieved with these structures, fabricating them needs complicated techniques, such as microfabrication or tapering. These will reduce the solidity of the whole structures and increase the cost of the devices. Simultaneously, these structures need special optical fibers, so the cost of devices is relatively high, especially for the PCF or WAF-based curvature sensors. In addition, the FBG- or LPG-based structures are very sensitive to temperature, which will lead to the cross sensitivity.

Recently, the singlemode-multimode-singlemode

(SMS) fiber structures have been investigated for various applications. They have the advantages of low cost and ease of fabrication. SMS fiber structures have been successfully utilized to sense temperature [17], refractive index (RI) [18], chemical concentration [19], strain [20], magnetic field [21-23] and curvature [24-26]. The fundamental principle of these applications is that the modes excited in the multimode fiber (MMF) section will interfere with each other and the effective RIs or energy of these excited modes could be influenced by the external environment/stimuli as well. When the SMS is bended, the effective RIs or energy of the excited modes will change. Hence, SMS fiber structures could also be used to sense curvature. In this work, we propose a highly sensitive optical fiber curvature sensor based on the cost-effective SMS fiber structure. Moreover, the sensor is almost temperature-independent.

## 2. Design and principle

The proposed SMS fiber structure and experimental setup are shown in Fig. 1. Our experimental SMS fiber structure consists of a piece of MMF whose two ends are fusion spliced to the single mode fibers (SMFs). The core and cladding diameters of the MMF are  $105 \mu\text{m}$  and  $125 \mu\text{m}$  (see Fig. 1(a)), respectively. In our experiments, we have fabricated two SMS structures with the MMF length  $L$  of 26 mm and 48 mm, respectively. The two ends of the sensing structures are fixed on two translation stages (see

Fig. 1(b)). By moving one stage, the separation distance between the two stages can be changed accurately and then the SMS structure is forced to curve. In this way, different curvatures could be applied on the fiber sensor. The fiber curvature is given by [27]

$$\rho = \frac{I}{R} = \frac{2(h_0 - h)}{(h_0 - h)^2 + a^2}, \quad (1)$$

where  $R$  is the curvature radius of the bending fiber,  $h_0$  and  $h$  are the heights of the unbent SMS structure and the center of the bent MMF section (see Fig. 1(b)),  $a$  is the half of the distance between the two clamps.

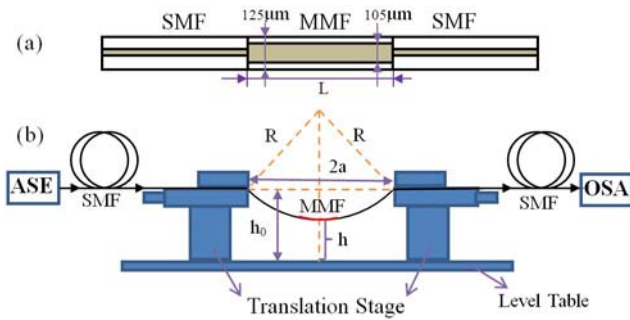


Fig. 1. SMS fiber structure (a) and experimental setup for studying the sensing properties of the system (b).

When the light from the wideband amplified spontaneous emission (ASE) light source passes through the lead-in SMF and enters into the MMF, the fundamental core mode  $LP_{01}$  spreads out widely and the high-order modes  $LP_{0j}$  are excited within the MMF. These high-order modes will interfere with each other and then be coupled into the core of the lead-out SMF. The transmission spectrum is monitored with the optical spectrum analyzer (OSA) and can be expressed as [28]

$$I(\lambda) = \sum_{i=1}^N \eta_i^2 \cdot I_0(\lambda) + \sum_{i \neq j=1}^N \eta_i \cdot \eta_j \cdot I_0(\lambda) \cdot \cos(2\pi \Delta n_{ij} L / \lambda) \quad (2)$$

where  $I_0$  is the intensity of the fundamental mode  $LP_{01}$  in the lead-in SMF and  $N$  is the total number of excited modes in the MMF.  $\eta_i$  and  $\eta_j$  are the coupling coefficients of the  $LP_{0i}$  and the  $LP_{0j}$  mode, respectively.  $\Delta n_{ij}$  is the effective RI difference between the involved interference modes. According to Eq. (2), the wavelength corresponding to the interference valley can be expressed by

$$\lambda_m = 2 \Delta n_{ij} L / (2m + 1), \quad (3)$$

where  $m$  is the interference order. When the curvature is applied, the corresponding force is exerted on the MMF, and the effective RIs of the modes will change. Besides, different modes will experience different index change due to their different mode field distribution. Therefore,  $\Delta n_{ij}$  will change with the curvature. This will result in the shift of interference valley wavelength with the curvature in the transmission spectrum, which can be employed for curvature sensing.

According to Eq. (2), the intensity of the interference valley is given by

$$I(\lambda_m) = \sum_{i=1}^N \eta_i^2 \cdot I_0(\lambda_m) - \sum_{i \neq j=1}^N \eta_i \cdot \eta_j \cdot I_0(\lambda_m). \quad (4)$$

The interference valley is more remarkable when the energy of the involved interference modes is closer. When the curvature of the SMS structure varies, the coupling coefficient  $\eta$  will change as well. Meanwhile, bending also alters the energy leakage of modes. Then, the energy of every mode and the energy difference between them will change due to the energy redistribution and leakage. Therefore, the intensity of the interference valley will also vary with the curvature, which can be employed for curvature sensing, too.

### 3. Results and discussion

Fig. 2 shows the transmission spectra of the proposed sensor with 26 mm-long MMF for the curvature ranging from 0.60 to 1.55  $m^{-1}$ . It is clear from Fig. 2 that the interference valley shifts to short wavelength side with curvature. The valley wavelength as a function of curvature is plotted in Fig. 3. Figs. 2 and 3 indicate that the total wavelength shift can reach up to 11.88 nm in the experimental curvature range. The valley wavelength has a good linear relationship with the curvature. The sensitivity is around -13.17  $nm/m^{-1}$ , which is about 3–4 times higher than those of the PCF-based bending sensors (4.451  $nm/m^{-1}$ , 3.046  $nm/m^{-1}$ ) [6, 8]. We call this kind of curvature sensor wavelength-shift-type sensor. For the 0.02 nm wavelength resolution of our OSA, the resolution of the curvature measurement is about  $1.5 \times 10^{-3} m^{-1}$ . We would like to point out that Silva et al. achieved 64.7  $nm/m^{-1}$  sensitivity in the curvature range of 1.28–1.52  $m^{-1}$  with a SMF-coreless MMF-SMF structure in 2012 [24]. The sensitivity is relatively high, but the linear response range is relatively small. Moreover, the sensing properties under small curvature (i.e.  $<1.28 m^{-1}$ ) were not investigated in Ref. 24.

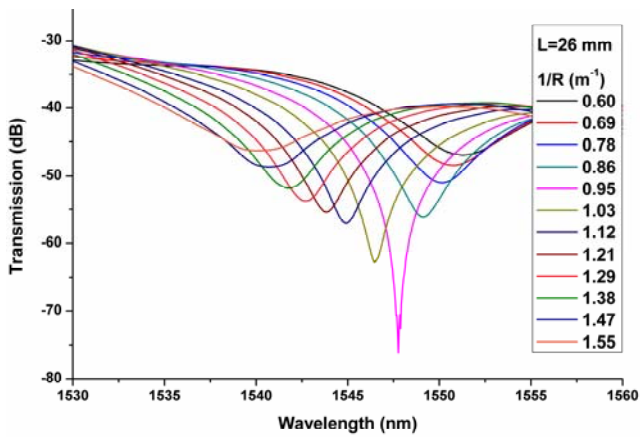


Fig. 2. Transmission spectra of the proposed sensor with 26 mm-long MMF for the curvature ranging from 0.60 to 1.55  $m^{-1}$ .

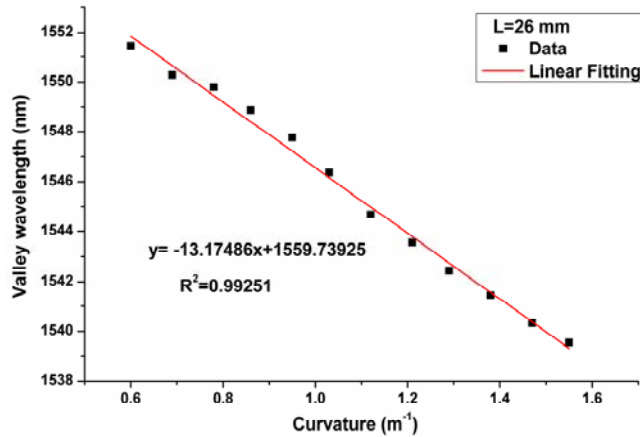


Fig. 3. Valley wavelength as a function of curvature for the structure with 26 mm-long MMF.

In addition to the wavelength shift with the curvature, the intensity corresponding to the valley wavelength varies with the curvature simultaneously (see Fig.2). Fig. 2 displays that the intensity of the interference valley decreases initially and then increases with the curvature in the range of 0.6-1.55  $m^{-1}$ . The minimum valley intensity happens for the structure with curvature of 0.95  $m^{-1}$ . For this structure, the shift of the valley wavelength is monotonously and linearly with the curvature in a wider curvature range, so the wavelength shift is more suitable for curvature sensing than the valley intensity variation.

For other certain structures (for example, the length of the MMF is appropriate), the applied microbend may have equal influence on the effective RI variation of the involved interference modes. So the effective RI difference between the interference modes would not

change with the curvature, and then the shift of the valley wavelength will be unobvious with curvature according to Eq. (3). We have verified this case with another SMS structure with 48 mm-long MMF section. Fig. 4 shows the corresponding transmission spectra under curvature ranging from 0 to 0.89  $m^{-1}$ . Two interference valleys are observed for this structure. The intensities of the interference valleys vary obviously with the curvature, but the valley wavelengths are almost independent of the curvature. The intensity of valley A decreases gradually with the curvature, while that of valley B increases gradually with the curvature. The explicit curvature-dependent intensities of valley A and valley B are depicted in Fig. 5. It is found that the intensity of valley A follows an exponential law with the curvature in the range of 0-0.89  $m^{-1}$ , whereas the intensity of valley B has a good linear relationship with the curvature in the range of 0.22-0.89  $m^{-1}$ . Therefore, the intensity variation of valley B with curvature may be more suitable for curvature sensing. The sensitivity of the intensity variation of valley B with curvature is about 24.64  $dB/m^{-1}$ , which is  $\sim 8.8$  times higher than that of the sensor based on tapered PCF-MZI structure (2.81  $dB/m^{-1}$ ) in the similar curvature range [7]. We call this kind of curvature sensor intensity-variation-type sensor. It is worth noting that Gong et al. have fabricated a curvature sensor with high sensitivity ( $\pm 130.37 dB/m^{-1}$ ) in the range of 0.11-0.34  $m^{-1}$  [26]. However, the corresponding monotonously linear response region is very small, which will limit its practical applications. As such, the highest sensitivity of our proposed structure is also larger than 100  $dB/m^{-1}$  in a narrow curvature range (see the curve of valley A at high curvature in Fig.5).

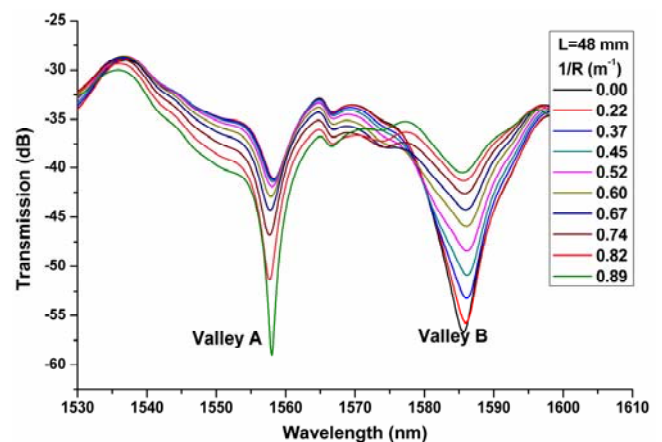


Fig. 4. Transmission spectra of the proposed sensor with 48 mm-long MMF under curvature ranging from 0 to 0.89  $m^{-1}$ .

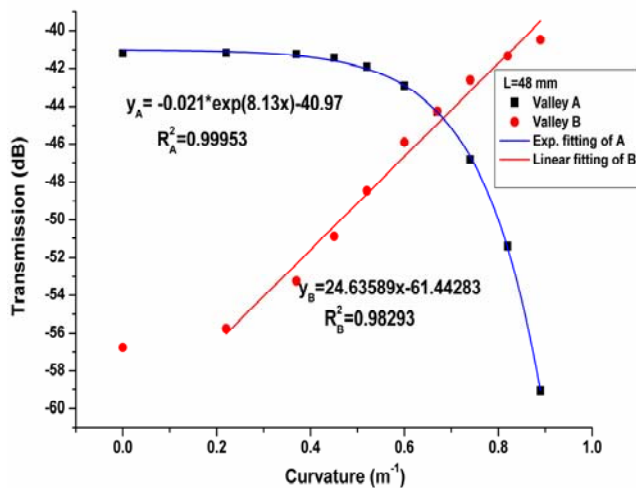


Fig. 5. Intensities of valley A and valley B as functions of curvature for the structure with 48 mm-long MMF.

Furthermore, our preliminary experiments show that the temperature sensitivities of the wavelength-shift-type and intensity-variation-type sensors are less than  $10 \text{ pm}/^\circ\text{C}$  and  $0.003 \text{ dB}/^\circ\text{C}$ , respectively. These are negligible when comparing with the curvature sensitivity, which may be assigned to the low thermal expansion coefficient and low thermo-optic coefficient of silica. Hence, the proposed sensors are temperature-insensitive when used as curvature sensors.

#### 4. Conclusions

In summary, a kind of curvature sensor based on SMS fiber structure is proposed. It was found that the interference valley wavelength of the SMS fiber structure with 26 mm-long MMF is highly sensitive to the bending. The shift of the valley wavelength has a good linear relationship with the curvature in the range of  $0.60\text{--}1.55 \text{ m}^{-1}$ . For this wavelength-shift-type curvature sensor, the obtained sensitivity is  $-13.17 \text{ nm}/\text{m}^{-1}$ . The temperature sensitivity is less than  $10 \text{ pm}/^\circ\text{C}$ , which is negligible. For the SMS fiber structure with 48 mm-long MMF, the valley wavelength is not sensitive to the bending, but the intensity of the interference valley varies with the curvature linearly in the curvature range of  $0.22\text{--}0.89 \text{ m}^{-1}$ . For this intensity-variation-type curvature sensor, the sensitivity is around  $24.64 \text{ dB}/\text{m}^{-1}$ . The temperature effect is very low (less than  $0.003 \text{ dB}/^\circ\text{C}$ ). Considering the easy fabrication and low cost of SMS fiber structures, the proposed structures are good candidates for the curvature sensing.

#### Acknowledgment

This research was supported by the Shanghai Natural Science Fund (No. 13ZR1427400), the Innovation Fund Project for Graduate Student of Shanghai (No. JWCXSL1302) and the Hujiang Foundation of China (B14004).

#### References

- [1] S. Dong, S. Pu, J. Huang, *Appl. Phys. Lett.* **103**, 111907 (2013).
- [2] S. Dong, S. Pu, H. Wang, *Opt. Express* **22**, 19108 (2014).
- [3] S. Pu, S. Dong, *IEEE Photonics J.* **6**, 5300206 (2014).
- [4] Y. Xu, Z. Gu, J. Chen, *J. Univ. Shanghai Sci. Technol.*, **27**, 215 (2005).
- [5] Y. Xu, Z. Gu, J. Chen, *J. Univ. Shanghai Sci. Technol.* **28**, 9 (2006).
- [6] H. Gong, H. Song, X. Li, J. Wang, X. Dong, *Sensor. Actuat. A-Phys.* **195**, 139 (2013).
- [7] K. Ni, T. Li, L. Hu, W. Qian, Q. Zhang, S. Jin, *Opt. Commun.* **285**, 5148 (2012).
- [8] M. Deng, C. P. Tang, T. Zhu, Y. J. Rao, *Opt. Commun.* **284**, 2849 (2011).
- [9] H. Gong, C. C. Chan, P. Zu, L. H. Chen, X. Dong, *Opt. Commun.* **283**, 3142 (2010).
- [10] O. Frazão, J. M. Baptista, J. L. Santos, P. Roy, *Appl. Opt.* **47**, 2520 (2008).
- [11] H. Song, H. Gong, K. Ni, X. Dong, *Sensor. Actuat. A-Phys.* **203**, 103 (2013).
- [12] H. J. Patrick, C. C. Chang, S. T. Vohra, *Electron. Lett.* **34**, 1773 (1998).
- [13] W. Shin, Y. L. Lee, B. A. Yu, Y. C. Noh, T. J. Ahn, *Opt. Commun.* **283**, 2097 (2010).
- [14] Y. X. Jin, C. -C. Chan, X. Dong, Y. F. Zhang, *Opt. Commun.* **282**, 3905 (2009).
- [15] L. Y. Shao, J. Albert, *Opt. Lett.* **35**, 1034 (2010).
- [16] S. Li, Z. Wang, Y. Liu, T. Han, Z. Wu, C. Wei, H. Wei, J. Li, W. Tong, *Opt. Lett.* **37**, 1610 (2012).
- [17] Q. Wu, Y. Semenova, A. M. Hatta, P. Wang, G. Farrell, *Electron. Lett.* **46**, 1129 (2010).
- [18] Q. Wang, G. Farrell, *Opt. Lett.* **31**, 317 (2006).
- [19] X. Lan, J. Huang, Q. Han, T. Wei, Z. Gao, H. Jiang, J. Dong, H. Xiao, *Opt. Lett.* **37**, 1998 (2012).
- [20] S. M. Tripathi, A. Kumar, R. K. Varshney, Y. B. P. Kumar, E. Marin, J.-P. Meunier, *J. Lightwave Technol.* **27**, 2348 (2009).
- [21] H. Wang, S. Pu, N. Wang, S. Dong, J. Huang, *Opt. Lett.* **38**, 3765 (2013).

- [22] Y. Chen, Q. Han, T. Liu, X. Lan, H. Xiao, *Opt. Lett.* **38**, 3999 (2013).
- [23] W. Lin, Y. Miao, H. Zhang, B. Liu, Y. Liu, B. Song, *Appl. Phys. Lett.* **103**, 151101 (2013).
- [24] S. Silva, E. G. P. Pachon, M. A. R. Franco, P. Jorge, J. L. Santos, F. X. Malcata, C. M. B. Cordeiro, O. Frazão, *J. Lightwave Technol.* **30**, 3569 (2012).
- [25] S. Silva, O. Frazão, J. Viegas, L. A. Ferreira, F. M. Araújo, F. X. Malcata, J. L. Santos, *Meas. Sci. Technol.* **22**, 085201 (2011).
- [26] Y. Gong, T. Zhao, Y. Rao, Y. Wu, *IEEE Photon. Technol. Lett.* **23**, 679 (2011).
- [27] H. Dobb, K. Kalli, D. J. Webb, *Electron. Lett.* **40**, 657 (2004).
- [28] J. Zhang, S. Peng, A compact SMS refractometer based on HF corrosion scheme, in Proceedings of IEEE Conference on Photonics and Optoelectronics, China, June 19-21, 2010.

---

\*Corresponding author: [shenglipu@gmail.com](mailto:shenglipu@gmail.com)  
[shlpu@usst.edu.cn](mailto:shlpu@usst.edu.cn)  
[zhuiguang0903@163.com](mailto:zhuiguang0903@163.com)